

## Eutrophication and temperature drive large variability in carbon dioxide from China's Lake Taihu

Qitao Xiao,<sup>1</sup> Hongtao Duan<sup>1,2\*</sup>, Boqiang Qin,<sup>3</sup> Zhenghua Hu,<sup>4</sup> Mi Zhang,<sup>4</sup> Tianci Qi,<sup>1</sup> Xuhui Lee<sup>5</sup>

<sup>1</sup>Key Laboratory of Watershed Geographic Sciences, Nanjing Institute of Geography and Limnology, Chinese Academy of Sciences, Nanjing, China

<sup>2</sup>College of Urban and Environmental Sciences, Northwest University, Xi'an, China

<sup>3</sup>Taihu Laboratory for Lake Ecosystem Research, State Key Laboratory of Lake Science and Environment, Nanjing Institute of Geography and Limnology, Chinese Academy of Sciences, Nanjing, China

<sup>4</sup>Yale-NUIST Center on Atmospheric Environment, International Joint Laboratory on Climate and Environment Change (ILCEC), Nanjing University of Information Science and Technology, Nanjing, China

<sup>5</sup>School of the Environment, Yale University, New Haven, Connecticut

### Abstract

Eutrophication and warming are changing the functioning of lake ecosystems, and their impacts on lake carbon dioxide (CO<sub>2</sub>) variability have received increasing attention. However, how eutrophication and warming change lakes' carbon cycle has not been determined. Here, the surface partial pressure of CO<sub>2</sub> (*p*CO<sub>2</sub>) and CO<sub>2</sub> flux in Lake Taihu, a large and eutrophic lake in eastern China, was investigated based on monthly samplings over a 24-yr period (1992–2015), during which the lake experienced profound anthropogenic and climate changes. The results showed that eutrophication caused by nutrient enrichment plays a role in three aspects: (1) nutrient concentrations controlled the CO<sub>2</sub> variability on decadal scales; (2) peak *p*CO<sub>2</sub> and CO<sub>2</sub> fluxes occurred in river mouths due to large external nutrient loading inputs; and (3) eutrophication effects on CO<sub>2</sub> varied among subzones, which was linked to external inputs and in-lake primary production. Meanwhile, temperature controls the seasonal variation in CO<sub>2</sub> by stimulating primary production, leading to significantly lower *p*CO<sub>2</sub> and CO<sub>2</sub> fluxes in warm seasons with algal blooms. Further analysis suggested that temperature effects varied spatially and temporally, high nutrient loading may confound the temperature effects via stimulating CO<sub>2</sub> production. To our knowledge, this study presents the longest field measurements (24 yr) of CO<sub>2</sub> from such large and ice-free freshwater lakes with monthly surveys, which may provide a powerful example to demonstrate that eutrophication and warming can shape CO<sub>2</sub> variability from a temporal perspective. Future studies should focus on the interactive warming and eutrophication effects to accurately predict future CO<sub>2</sub> emission.

Inland waters (e.g., lakes, reservoirs, rivers, and shallow ponds) emit large amounts of carbon dioxide (CO<sub>2</sub>) into the atmosphere, which must be considered in the global CO<sub>2</sub> budget estimation (Cole et al. 2007; Tranvik et al. 2009; Raymond et al. 2013). Understanding the magnitude of CO<sub>2</sub> emissions from lakes is challenging due to large temporal–spatial variability, and identifying the factors driving the variability is essential to being able to predict the change of lake CO<sub>2</sub> flux. Given the lake CO<sub>2</sub> variability is related to multiple, interconnected physical, chemical, and biological processes, long-term (multidecades) observations are projected to shed light on the regulation of lake CO<sub>2</sub> from unique perspectives

(Davidson et al. 2015; Seekell and Gudas 2016; Finlay et al. 2019). However, only a few long-term continuous data series (more than 10 yr) have been reported until now, which may seriously hamper the understanding of lake contributions to the carbon cycle and predicts lake CO<sub>2</sub> responses to future environmental change (Perga et al. 2016; Seekell and Gudas 2016).

Eutrophication is widespread in inland lakes and its effects on lake CO<sub>2</sub> variability has received growing attentions. Most studies have shown that nutrient levels and algal blooms in eutrophic lakes are closely linked to CO<sub>2</sub> production and consumption, and have the potential to regulate the CO<sub>2</sub> temporal–spatial variability (Davidson et al. 2015; Xiao et al. 2020a; Morales-Williams et al. 2021). For example, nutrient enrichment can increase CO<sub>2</sub> production and emission via stimulating respiration (Kortelainen et al. 2006; Wang et al. 2017) and methane oxidation (Bastviken et al. 2002;

\*Correspondence: htduan@niglas.ac.cn

Additional Supporting Information may be found in the online version of this article.

Denfeld et al. 2016). On the other hand, algal blooms in eutrophic lakes can consume CO<sub>2</sub> and decrease emissions due to high primary production (Balmer and Downing 2011; Pacheco et al. 2014). It is well known that nutrient enrichment controlled algal blooms in eutrophic lakes, the complexity of intertwined processes between nutrient and primary production led to uncertain eutrophication effects on lake CO<sub>2</sub> variability. Considering lake eutrophication has increased globally (Ho et al. 2019), the relative influence of these variables on CO<sub>2</sub> variability in eutrophic lakes should be considered to better understand the effects of eutrophication.

Biogeochemical processes controlling lake CO<sub>2</sub> variability, such as metabolism, are generally temperature dependent. Lakes are sensitive to climate change, and lake water temperatures have increased worldwide due to climate warming (Woolway et al. 2020). Warming of the water may affect the functions of lake ecosystems by altering physical processes (e.g., the duration of ice cover), biological processes (e.g., the abundance of primary producers), and chemical processes (e.g., the mineralization of organic matter), which are associated with CO<sub>2</sub> variability (Kosten et al. 2010; Davidson et al. 2015; Finlay et al. 2015). However, predicting the change of lake CO<sub>2</sub> under climate warming is difficult mostly due to the uncertain temperature effects. Specifically, rising temperature has been shown to increase, decrease, or have neutral effect on lake CO<sub>2</sub> level (Sobek et al. 2005; Kosten et al. 2010; Finlay et al. 2015). Meanwhile, lake warming is accelerating eutrophication (Kosten et al. 2012; Paerl and Paul 2012; Ho et al. 2019); however, there is little information on how eutrophication and increasing temperatures will combine to affect current and future lake CO<sub>2</sub> emissions.

Lake Taihu, the third-largest freshwater lake (area 2338 km<sup>2</sup>) in China, has suffered serious eutrophication issues with nutrient enrichment due to rapid population and economic growth since the 1990s (Duan et al. 2009; Qin et al. 2019; Qi et al. 2020). Currently, eco-environmental issues, such as frequent algal bloom events together with climate change, have made the lake a typical research site for ecologists, limnologists, and environmentalists around the world (Paerl et al. 2011; Lee et al. 2014; Qin et al. 2019). However, much of these work paid little attention on the drivers of the lake surface CO<sub>2</sub> variability, leading to the effects of eutrophication and climate change on CO<sub>2</sub> flux still unclear. Profound environmental changes in Lake Taihu, such as increasing temperature and decreasing pollutant loadings, have occurred over the past 30 yr (Xu et al. 2017; Zhang et al. 2018a; Qin et al. 2019). Although the correlations between algal blooms and pollutant loadings are analyzed (Xu et al. 2017), studies have shown that climate warming has boosted algal growth in Lake Taihu (Duan et al. 2009; Zhang et al. 2018a; Qin et al. 2019). Both of these factors provide a unique opportunity to generalize the effects of local changes on lake CO<sub>2</sub> and to predict lake CO<sub>2</sub> responses to environmental changes.

In the present study, we report the results of the pCO<sub>2</sub> of Lake Taihu over a 24-yr period (1992–2015) on a monthly scale. Using long-term (1992–2015) records on a monthly scale, the objectives were to: (1) characterize the pCO<sub>2</sub> variability of a large and eutrophic lake at different temporal–spatial scales and (2) elucidate the role of eutrophication and climate change in shaping lake CO<sub>2</sub>. This work, to the best of the authors' knowledge, has the longest field records of pCO<sub>2</sub> from large and ice-free lakes in subtropical climates at such high temporal scales in the published literature around the world. We believe this study not only improves the understanding of the CO<sub>2</sub> cycling of freshwater lakes but also presents a powerful data set to evaluate the CO<sub>2</sub> response to lake environmental change from a temporal perspective.

## Materials and methods

### Study region and sampling site

The Lake Taihu catchment, with an area of 36,500 km<sup>2</sup>, is located in the southeastern part of the Yangtze River Delta of eastern China (Fig. 1). The catchment has nearly 200 rivers and canals connected to the lake without winter ice cover. The anthropogenic pollutant discharge into the lake through inflow rivers has been shown to be high but strongly variable among years; for example, the total nitrogen (TN) input decreased from  $7.55 \times 10^4$  t in 1994 to  $3.87 \times 10^4$  t in 2015 (Qin et al. 2007; Xiao et al. 2019). The local region features a subtropical climate with a low water temperature (monthly mean: 3.9°C) and precipitation (monthly mean: 60 mm) in winter and a peak (water temperature: 31°C; precipitation: 170 mm) in summer (Xiao et al. 2017). The annual precipitation and air temperature are approximately 1100 mm and 16.2°C (Lee et al. 2014), respectively.

Sampling sites were situated in northern and central parts of the lake and are connected to the Zhihu Gang, Wujing Gang, and Liangxi River (Fig. 1), the three main inflowing rivers around the lake. The catchments of Zhihu Gang and Wujing Gang contain a large number of factories (Xu et al. 2017). The Liangxi River passes through Wuxi, a highly industrialized city with an urban population of more than 4 million (Xu et al. 2017; Xiao et al. 2020b). Substantial pollutants from domestic sewage, industrial activities, and agricultural activities are discharged into the three rivers that then flow into the lake. There were seven sampling sites that were evenly spatially distributed (Fig. 1).

### Data acquisition and calculations

Field samplings and surveys of Lake Taihu represent one of the earliest typical freshwater lake observations in China. The long-term (1992–2015) observation data were provided by TLLER (the Taihu Laboratory for Lake Ecosystem Research). TLLER aimed to understand the patterns, processes, and mechanisms of freshwater lake change and was a long-term lake ecosystem observation station of Chinese Ecosystem Research Network. Systematic and complete observations of the

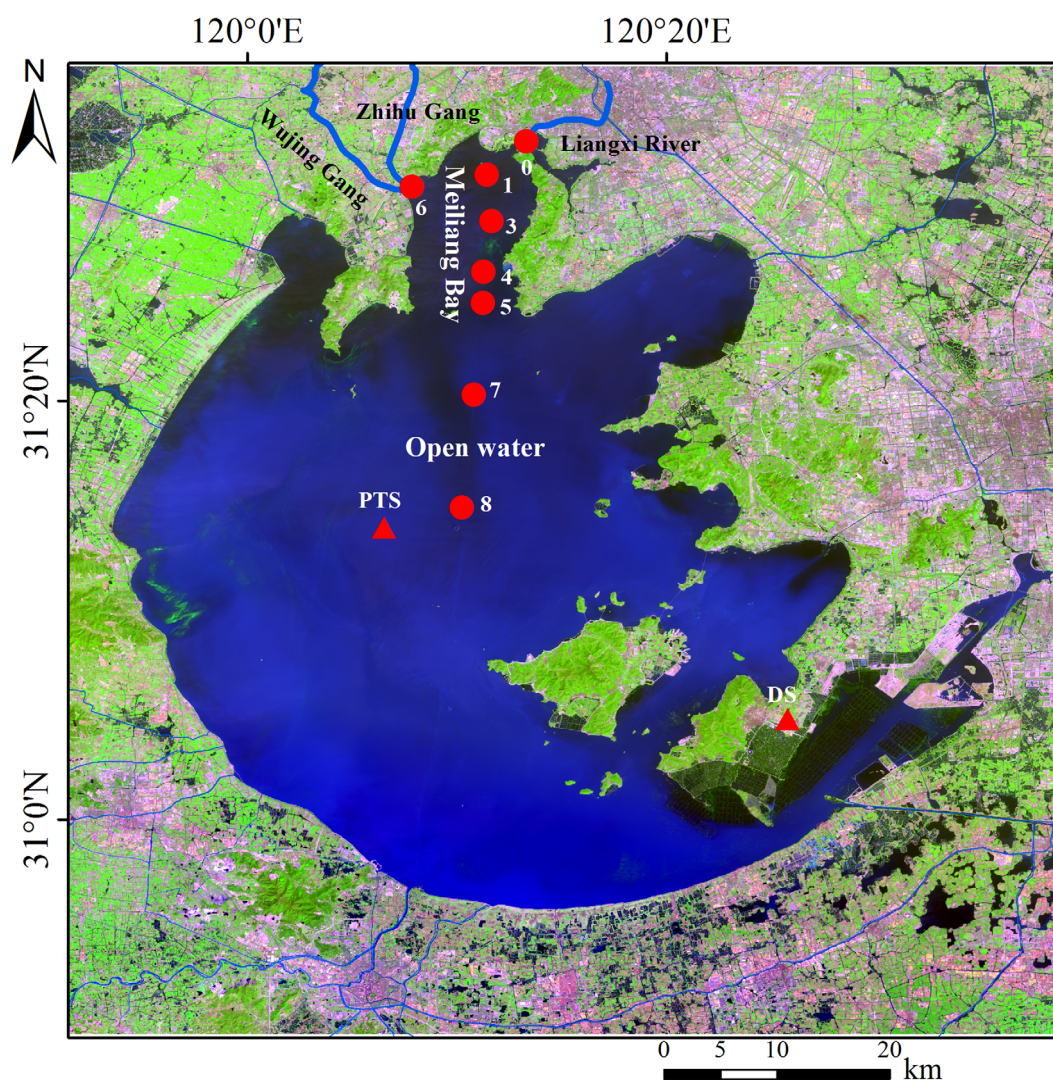


**Fig. 1.** Location of sampling sites and the three main inflowing rivers (Wujing Gang, Zhihu Gang, and Liangxi River) in Lake Taihu. The sites were divided into three groups based on external loadings input and eutrophic status, the river mouth inflow (the site of #0 and #6), Meiliang Bay (the sites of #1, #3, #4, and #5), and the open water (the sites of #7 and #8). The triangles indicate the micrometeorological sites, including lake PTS and land DS.

environmental variables of large eutrophic lakes, including physical, chemical, and biological parameters, have been carried out monthly by TLLER researchers since 1992.

The environmental variables considered in the present study were nutrients (TN, total phosphorus [TP], ammonium nitrogen [ $\text{NH}_4^+\text{-N}$ ], and nitrate nitrogen [ $\text{NO}_3^-\text{-N}$ ]), pH, dissolved oxygen (DO), water temperature ( $T_w$ ), alkalinity (Alk), chlorophyll *a* (Chl *a*), dissolved organic carbon (DOC), and water clarity. The sampling and measurements of these variables have been previously reported in detail, including the detection limit and precision for these environmental variables (Xu et al. 2017; Zhang et al. 2018a; Xiao et al. 2020b). Specifically, the detection limit for  $\text{NH}_4^+\text{-N}/\text{NO}_3^-\text{-N}$  and DOC were 0.6 and 0.4  $\mu\text{g L}^{-1}$ , respectively. Long-term (1992–2015) meteorological data, such as air temperature and wind speed,

were obtained from the DS station (Fig. 1) of the China Meteorological Observation Network.

The  $p\text{CO}_2$  was calculated according to the measurements of pH, Alk, and  $T_w$  of the lake, and our study shows the calculation processes in detail in the Supporting Information (Text S1). In the published literature, most lake  $p\text{CO}_2$  is calculated from  $T_w$ , pH, and Alk (Raymond et al. 2013; Abril et al. 2015; Weyhenmeyer et al. 2015). Additionally, the probe with a precision of  $\pm 0.01$  units for pH measurement in the field was carefully calibrated prior to sampling, and Alk was measured on the sampling day with a precision of  $\pm 0.5\%$ . Meanwhile, it should be noted that only few samples had a pH below 7 in this study, and the DOC concentration was relatively low (Table S1). Based on these pH and DOC levels, the uncertainties in lake  $p\text{CO}_2$  calculation are considered minor (Abril et al. 2015).

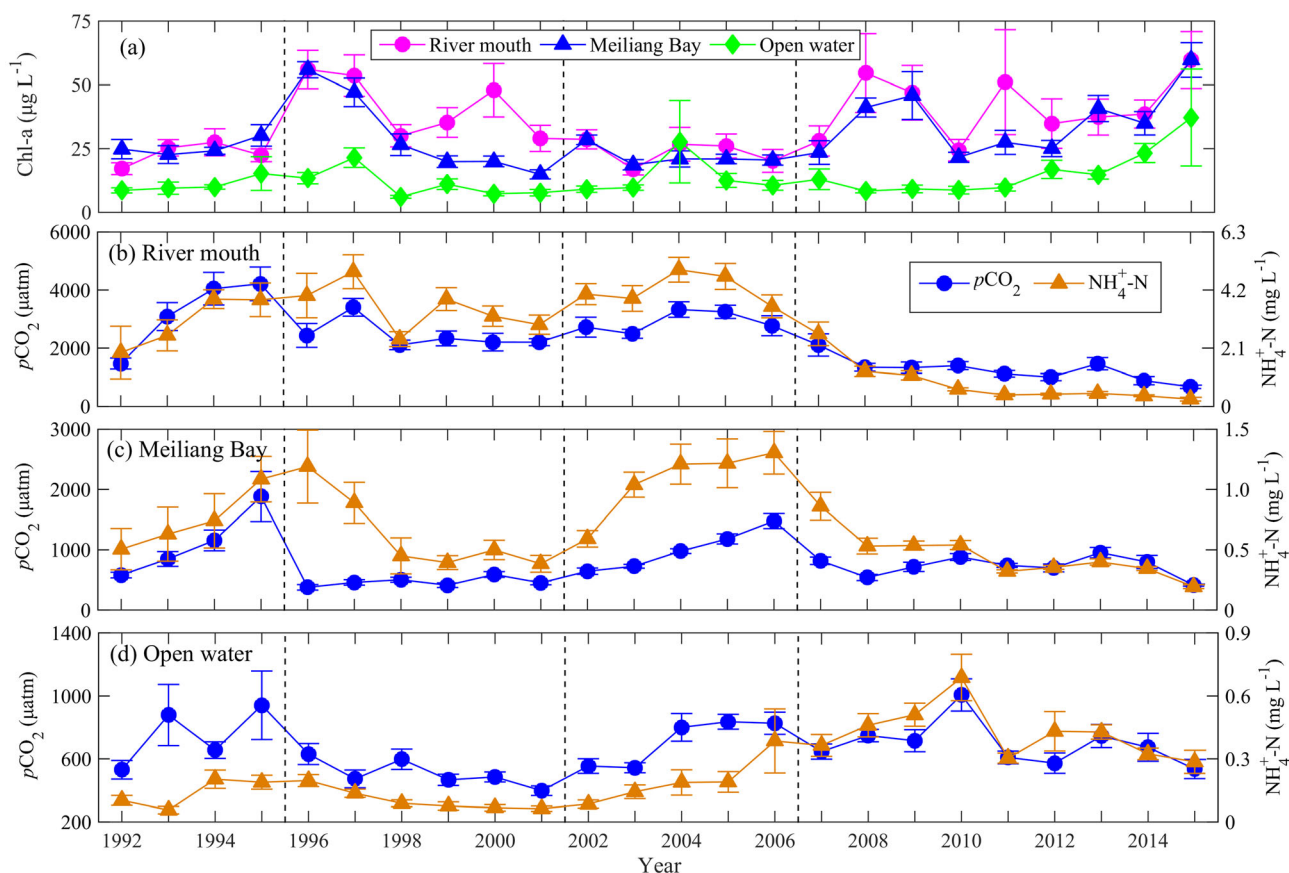


**Fig. 2.** Annual trend of Chl *a*, nutrient concentration ( $\text{NH}_4^+\text{-N}$  as an example), and  $p\text{CO}_2$  in the three subzones (river mouth, Meiliang Bay, and open water) from 1992 to 2015: **(a)** Chl *a* in the three subzones, **(b)** nutrient concentration and  $p\text{CO}_2$  in the river mouth, **(c)** nutrient concentration and  $p\text{CO}_2$  in Meiliang Bay, and **(d)** nutrient concentration and  $p\text{CO}_2$  in open water. Error bars indicate standard errors, and the dashed lines show the turning points for  $p\text{CO}_2$  in Lake Taihu.

The  $\text{CO}_2$  exchange flux across the lake-air interface ( $F_c$ ) was calculated using the diffusion model (Cole and Caraco 1998):

$$F_c = k \times K_H \times (p\text{CO}_2 - p_a) \quad (1)$$

where  $K_H$  denotes the  $\text{CO}_2$  Henry's constant (Text S1),  $p_a$  is the local atmosphere  $\text{CO}_2$  mixing ratio and was measured by a carbon dioxide gas analyzer (Xiao et al. 2014), and  $k$  is the  $\text{CO}_2$  gas exchange velocity across the lake-air interface. The equations for the  $k$  calculation are shown in detail in the Supporting Information (Text S2). A positive value of  $F_c$  indicates the lake emissions of  $\text{CO}_2$  to the atmosphere.

To assess the trophic status of the lake and its effect on  $\text{CO}_2$  dynamics, the trophic state index (TSI) was calculated (Text S3) from four major water quality parameters (Zhang et al. 2018b).

### Statistical analysis

We divided the sites into three subzones (Meiliang Bay, open water, and river mouth) according to geographic differences in eutrophic status and pollutant loadings. Meiliang

Bay, located in the northern part of the lake, is a semi-enclosed bay and is eutrophic due to nutrient enrichment. There are four sampling sites (#1, #3, #4, and #5) that are evenly distributed in the subzone. Open water, including sites #7 and #8 in the central zone of the lake, has lower eutrophication. The river mouth (sites #0 and #6) near the three inflowing rivers had the highest pollutant concentrations due to direct external input. The large differences in the mean concentrations of TN (river mouth:  $5.5 \text{ mg L}^{-1}$ ; Meiliang Bay:  $3.1 \text{ mg L}^{-1}$ ; open water:  $2.3 \text{ mg L}^{-1}$ ) and Chl *a* (river mouth:  $35.2 \text{ } \mu\text{g L}^{-1}$ ; Meiliang Bay:  $30.1 \text{ } \mu\text{g L}^{-1}$ ; open water:  $13.6 \text{ } \mu\text{g L}^{-1}$ ; Table S1) support the division of the study region.

For temporal analysis, subzonal mean environmental variables and  $\text{CO}_2$  were used. These subzonal mean values were calculated for each sampling using all data within the corresponding subzone from 1992 to 2015. In total, there were 288 data sets (12 months  $\times$  24 yr) for the analysis at each subzone. Monthly subzonal mean variables, including environmental variables and carbon ( $p\text{CO}_2$  and  $\text{CO}_2$  flux), were then calculated as the mean values for spring (March–May), summer (June–August), autumn (September–November), winter (December–February in

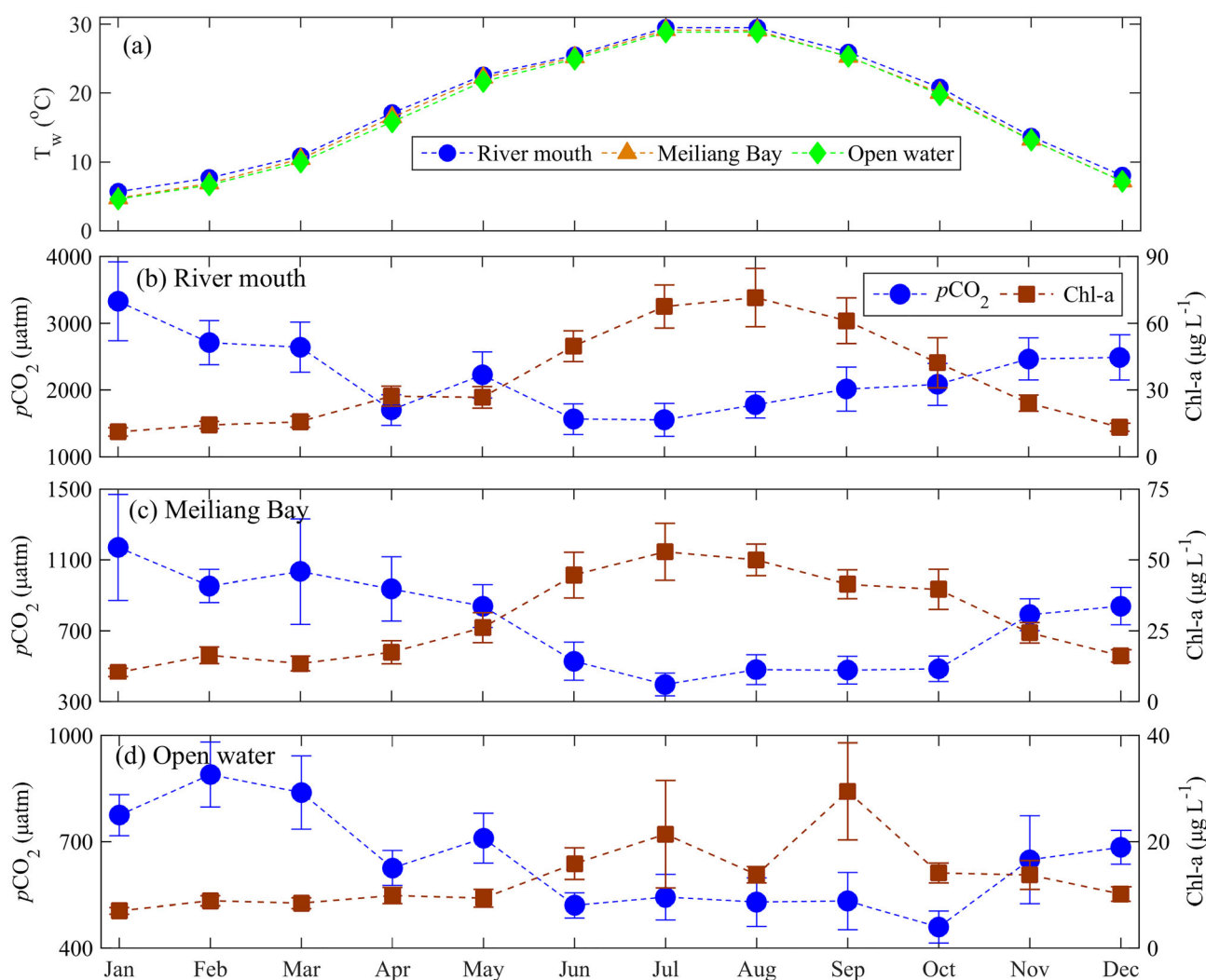


**Fig. 3.** Monthly mean water temperature,  $pCO_2$ , and Chl *a* concentrations in the three subzones (river mouth, Meiliang Bay, and open water) during the sampling period: (a) water temperature in the three subzones; (b)  $pCO_2$  and Chl *a* in the river mouth; (c)  $pCO_2$  and Chl *a* in Meiliang Bay, and (d)  $pCO_2$  and Chl *a* in open water. Error bar indicates one standard error. The relationships between the  $pCO_2$  and Chl *a* in the river mouth, Meiliang Bay, and open water are shown in Fig. 4.

the next year), and annual average values from 1992 to 2015. To determine the differences among the variables, the least significant difference test was performed, and statistically significant differences between variables were determined at  $p < 0.05$ .

## Results

### Annual trends of environmental variables

Significant warming and decreasing trends in wind speed were recorded over the lake from 1992 to 2015 (Fig. S1). The warming rate and decreasing rate of wind speed of the yearly measurements at DS station were  $0.35^\circ\text{C}$  per decade and  $0.27\text{ m s}^{-1}$  per decade, respectively. The annual trend of lake water temperature exhibited the same pattern (Fig. S1b). The

mean water temperature was  $17.5^\circ\text{C}$ , showing no spatial variability across the three subzones (Table S1).

The annual mean Chl *a* and nutrient concentrations varied significantly (Figs. 2a, S2). The Chl *a* concentration showed an increasing trend from 1992 to 1997 in both subzones and decreased between 1997 and 2007, except for a peak occurring in 2000 at the river mouth. After 2007, the Chl *a* concentration increased, with a peak occurring in 2015. The interannual variations in nutrient concentrations, such as TN, TP, and  $\text{NH}_4^+\text{-N}$ , can be divided into four stages in three subzones: (1) from 1992 to 1996 or 1997, the concentrations increased rapidly; (2) from 1996 or 1997 to 2001, the concentrations decreased; (3) from 2001 to 2006, the concentrations increased except for the TP in the river mouth; and (4) after 2006, the concentrations, not including those in open water, decreased rapidly,

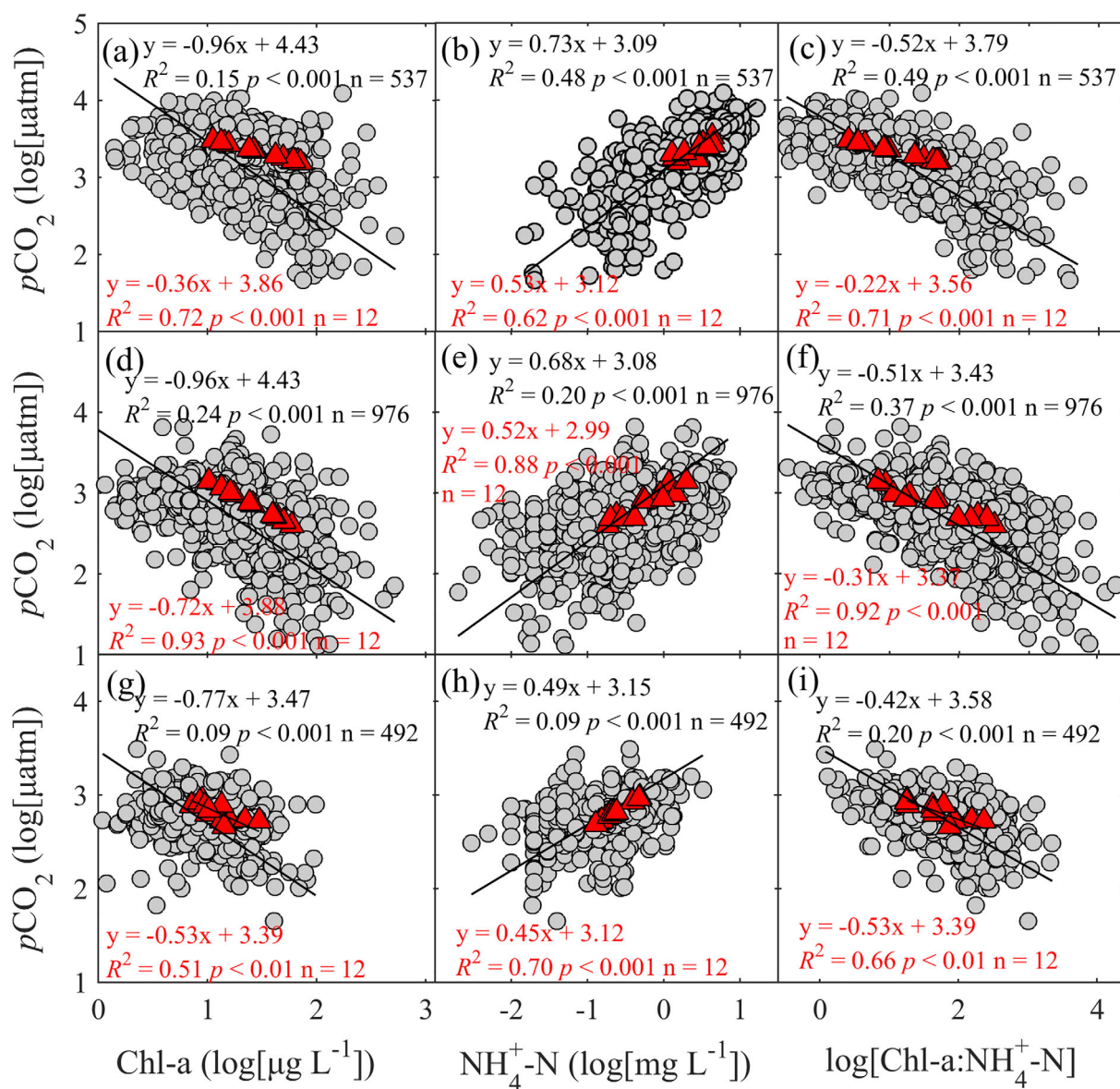


**Fig. 4.** Relationships between  $p\text{CO}_2$  and Chl  $a$ ,  $\text{NH}_4^+\text{-N}$  and the ratio of Chl  $a$  ( $\mu\text{g L}^{-1}$ ) to  $\text{NH}_4^+\text{-N}$  ( $\text{mg L}^{-1}$ ; Chl  $a$ :  $\text{NH}_4^+\text{-N}$ ) in the river mouth (a–c), Meiliang Bay (d–f), and open water (g–i) based on the long-term (1992–2015) measurements. Red triangles indicate the monthly mean values, and gray points indicate all data during the sampling period from 1992 to 2015.

with the lowest values occurring in approximately 2015. The open water was less affected by riverine pollutant discharge compared to the river mouth and Meiliang Bay, as shown by significantly ( $p < 0.01$ ) lower nutrient and Chl  $a$  concentrations (Table S1).

#### Interannual and monthly variabilities of $p\text{CO}_2$

The  $p\text{CO}_2$  showed substantial interannual variations (Fig. 2). Similar to the trends of the nutrients, the  $p\text{CO}_2$  interannual variations in the three subzones can also be divided into four stages: (1) from 1992 to 1995, the annual mean  $p\text{CO}_2$  increased rapidly, with peaks occurring in 1995 (river

mouth: 4213  $\mu\text{atm}$ ; Meiliang Bay: 1883  $\mu\text{atm}$ ; open water: 941  $\mu\text{atm}$ ); (2) from 1996 to 2001,  $p\text{CO}_2$  declined to approximately 2448  $\mu\text{atm}$  in the river mouth, 466  $\mu\text{atm}$  in Meiliang Bay, and 508  $\mu\text{atm}$  in open water; (3) from 2002 to 2006,  $p\text{CO}_2$  increased significantly in Meiliang Bay and open water and fluctuated at approximately 2900  $\mu\text{atm}$  in the river mouth; and (4) after 2007,  $p\text{CO}_2$  decreased rapidly in the river mouth and Meiliang Bay, with the lowest values occurring in 2015, but  $p\text{CO}_2$  increased to a peak in 2010 and then declined in open water.

The lake exhibited remarkable seasonal variations in  $p\text{CO}_2$ , with low values occurring in the warm season and high values

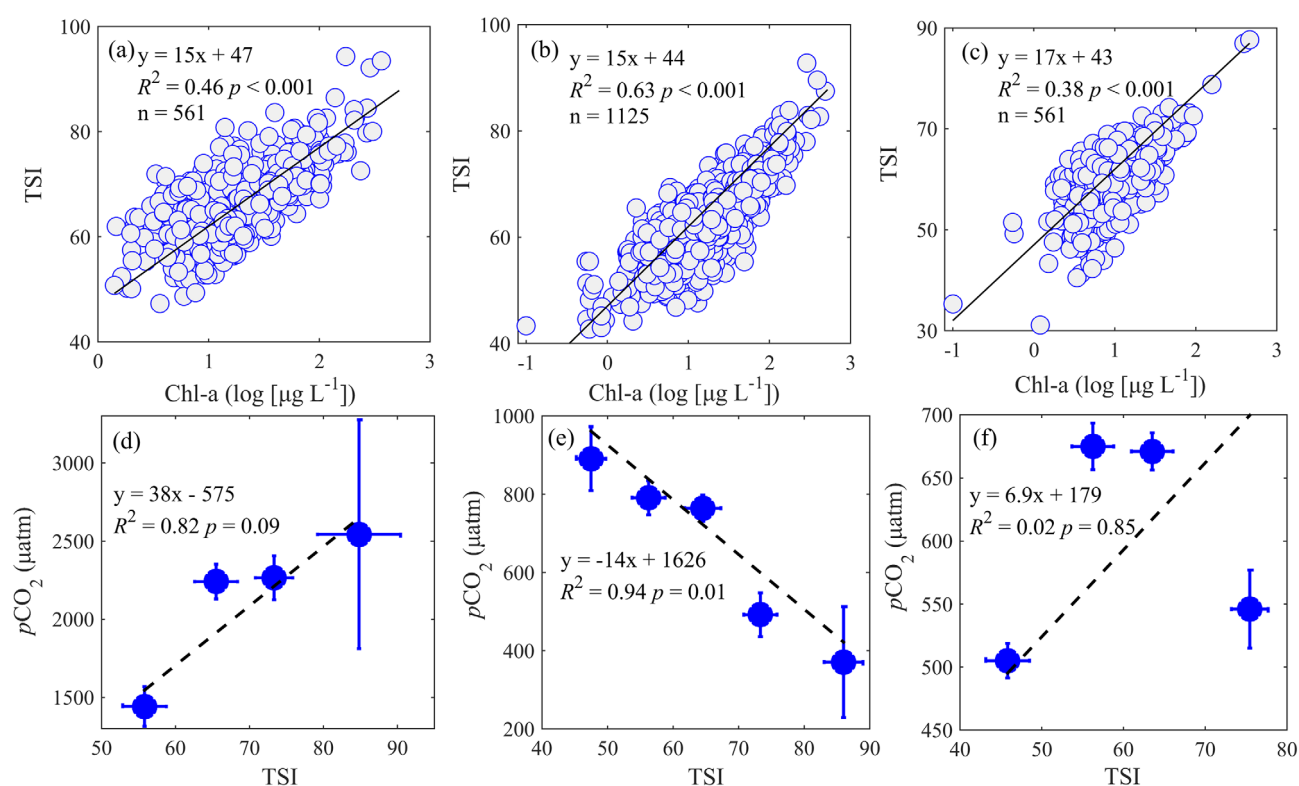


**Fig. 5.** Relationships between Chl *a* and TSI in (a) river mouth, (b) Meiliang Bay, and (c) open water, and relationships between bin average  $p\text{CO}_2$  and TSI in (d) river mouth, (e) Meiliang Bay, and (f) open water. Error bars indicate one standard error (vertical) or standard deviation (horizontal).

occurring in the cold season (Fig. 3). Seasonal variations in the water temperature were highly consistent across the three subzones (Fig. 3a); however, the  $p\text{CO}_2$  seasonal patterns varied among subzones. Specifically, seasonal variation in  $p\text{CO}_2$  was more remarkable in subzones with high Chl *a* (river mouth and Meiliang Bay) than in open water with low Chl *a*. Meanwhile, the  $p\text{CO}_2$  seasonal patterns varied among the four periods (1992–1995, 1996–2001, 2002–2006, and 2007–2015) in each subzone, although the seasonal patterns in water temperature and Chl *a* were consistent across the four periods (Fig. S3). Specifically, more profound seasonal variation in  $p\text{CO}_2$  was found during 1996–2001 than during 1992–1995 and during 2007–2015 in each subzone, and seasonal variation was not evident during 2002–2006.

Further analysis showed that  $p\text{CO}_2$  generally peaked in winter. In the river mouth, the annual mean  $p\text{CO}_2$  in winter ( $2843 \pm 437 \mu\text{atm}$ ) was significantly ( $p < 0.05$ ) greater than the mean in spring ( $2189 \pm 472 \mu\text{atm}$ ), summer ( $1631 \pm 126 \mu\text{atm}$ ), and autumn ( $2187 \pm 244 \mu\text{atm}$ ), and the  $p\text{CO}_2$  in the spring, summer, and autumn showed insignificant ( $p > 0.05$ ) differences. In Meiliang Bay, the mean  $p\text{CO}_2$  in spring ( $937 \pm 97 \mu\text{atm}$ ) and winter ( $988 \pm 168 \mu\text{atm}$ ) was approximately twice that in summer ( $468 \pm 67 \mu\text{atm}$ ) and autumn ( $585 \pm 179 \mu\text{atm}$ ). In open water, the mean  $p\text{CO}_2$  in spring ( $725 \pm 108 \mu\text{atm}$ ) and winter ( $783 \pm 103 \mu\text{atm}$ ) was also

higher than that in summer ( $531 \pm 12 \mu\text{atm}$ ) and autumn ( $545 \pm 96 \mu\text{atm}$ ), with significant ( $p < 0.05$ ) differences.

#### Effects of environmental variables on the $p\text{CO}_2$ variations

The  $p\text{CO}_2$  was negatively correlated with biological variables (the Chl *a* in our study) and positively correlated with nutrients based on the long-term observations across sites and time in the three subzones (Fig. 4). Chl *a* indicated primary production in the eutrophic lake and affected the  $p\text{CO}_2$  seasonal variation, and the negative correlations between  $p\text{CO}_2$  and Chl *a* were more significant in the river mouth and Meiliang Bay than in open water (Fig. 4a,d,g). The  $p\text{CO}_2$  of open water was also less influenced by nutrients ( $\text{NH}_4^+\text{-N}$  as an example of the study). Additionally, the  $p\text{CO}_2$  was negatively correlated with the ratio of Chl *a* to  $\text{NH}_4^+\text{-N}$  (Fig. 4c,f,i).

The subzonal  $p\text{CO}_2$  exhibits different responses to eutrophication status (Fig. 5). The TSI was used to assess the eutrophication status, which was associated with Chl *a* (Fig. 5a–c). The annual mean TSI with values larger than 50 (Table S1) indicated that the three subzones were eutrophic. The  $p\text{CO}_2$  increased with increasing TSI in the river mouth with high river pollutant discharge (Fig. 5d) but decreased with increasing TSI in Meiliang Bay with frequent algal blooms (Fig. 5e). A neutral influence of TSI on  $p\text{CO}_2$  was found in open water with lower eutrophication (Fig. 5f).

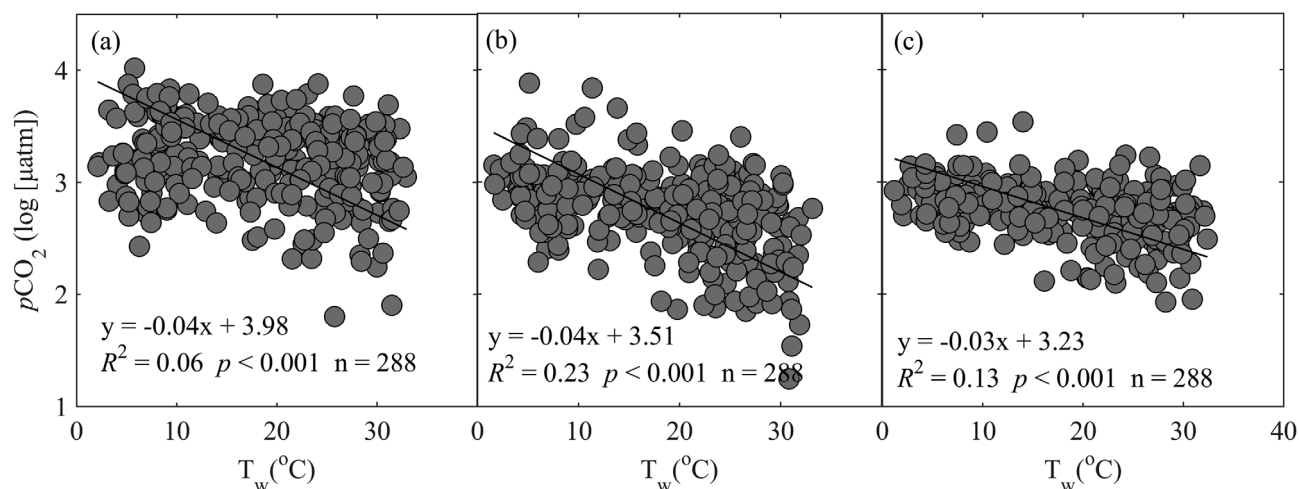


**Fig. 6.** Correlations between monthly  $p\text{CO}_2$  and water temperature in (a) the river mouth, (b) Meiliang Bay, and (c) open water based on long-term (1992–2015) sampling.

**Table 1.** Linear regression equation between normalized monthly mean  $p\text{CO}_2$  ( $y$ ,  $\mu\text{atm}$ ) and water temperature ( $x$ ,  $^{\circ}\text{C}$ ) among different periods (1992–1995, 1996–2001, 2002–2006, and 2007–2015, and the full period (1992–2015)) in the three subzones. The period division was based on the annual trend in  $p\text{CO}_2$  as shown in Fig. 2.

	River mouth	Meiliang Bay	Open water
1992–1995	$y = -0.03x + 3.89$ , $R^2 = 0.41$ , $p < 0.05$	$y = -0.05x + 3.57$ , $R^2 = 0.78$ , $p < 0.01$	$y = -0.03x + 3.26$ , $R^2 = 0.58$ , $p < 0.01$
1996–2001	$y = -0.01x + 3.60$ , $R^2 = 0.61$ , $p < 0.01$	$y = -0.02x + 3.01$ , $R^2 = 0.86$ , $p < 0.01$	$y = -0.02x + 2.96$ , $R^2 = 0.69$ , $p < 0.01$
2002–2006	$y = -0.01x + 3.69$ , $R^2 = 0.16$ , $p = 0.20$	$y = -0.01x + 3.18$ , $R^2 = 0.40$ , $p < 0.05$	$y = -0.01x + 3.03$ , $R^2 = 0.08$ , $p = 0.38$
2007–2015	$y = -0.01x + 3.30$ , $R^2 = 0.48$ , $p < 0.05$	$y = -0.02x + 3.15$ , $R^2 = 0.52$ , $p < 0.05$	$y = -0.01x + 3.02$ , $R^2 = 0.29$ , $p < 0.05$
1992–2015	$y = -0.01x + 3.55$ , $R^2 = 0.74$ , $p < 0.01$	$y = -0.02x + 3.16$ , $R^2 = 0.76$ , $p < 0.01$	$y = -0.01x + 2.98$ , $R^2 = 0.62$ , $p < 0.01$

The  $p\text{CO}_2$  decreased with increasing water temperature (Fig. 6; Table 1). However, both analyses showed that the correlations between water temperature and temperature varied spatially and temporally. Spatially, the highest correlation was generally found in Meiliang Bay, suggesting a relatively high temperature dependency of  $p\text{CO}_2$  in the eutrophic subzone with algal blooms. Temporally, the highest correlation was found in 1996–2001, during which nutrient loadings were low. Meanwhile, less temperature dependency was found in eutrophic river mouths with significant external loading inputs. It should be noted that the correlations between  $p\text{CO}_2$  and temperature were positively correlated with the ratio of Chl *a* to TN and negatively correlated with the ratio of TN to TP (Fig. S4).

The variability in annual  $p\text{CO}_2$  was positively correlated with  $\text{NH}_4^+\text{-N}$  and TN, especially for river mouths (Fig. 2; Table S2). Significant negative correlations between  $p\text{CO}_2$  and Chl *a* were found in the river mouth and Meiliang Bay, and the annual  $p\text{CO}_2$  in river mouth was negatively correlated with DO in the river mouth. It should be noted that the annual  $p\text{CO}_2$  variability were not related to temperature in the three sub-zones (Figs. 2, S1; river mouth:  $r = 0.03$ ,  $p = 0.89$ ; Meiliang Bay:  $r = 0.14$ ,  $p = 0.53$ ; open water:  $r = 0.06$ ,

$p = 0.77$ ). Meanwhile, the measurements of DOC were conducted from 2004 to 2015, and analysis using the correlation between annual variation in DOC and annual variability in  $p\text{CO}_2$  reveals a strong relationship between DOC and  $p\text{CO}_2$  in river mouth (Table S2).

#### $p\text{CO}_2$ and $\text{CO}_2$ flux

The mean  $p\text{CO}_2$  in Meiliang Bay ( $785 \pm 360 \mu\text{atm}$ ) and open water ( $661 \pm 160 \mu\text{atm}$ ) was significantly ( $p < 0.01$ ) lower than that in the river mouth ( $2225 \pm 993 \mu\text{atm}$ ) during the sampling period, and the average  $p\text{CO}_2$  was  $1224 \pm 869 \mu\text{atm}$  across the three subzones. The  $\text{CO}_2$  exchange flux between the lake–air interface was calculated via the equation above. The  $\text{CO}_2$  flux varied spatially, annually, and seasonally, which was consistent with the  $p\text{CO}_2$ . Spatially, peak  $\text{CO}_2$  emission flux occurred in the river mouth (annual mean value:  $93.6 \pm 48.6 \text{ mmol m}^{-2} \text{ d}^{-1}$ ; Fig. S5). For comparison, the annual mean  $\text{CO}_2$  emission fluxes in Meiliang Bay and open water were  $20.0 \pm 22.3$  and  $12.7 \pm 8.8 \text{ mmol m}^{-2} \text{ d}^{-1}$ , respectively. Annually, the  $\text{CO}_2$  emission flux showed substantial variations in both subzones (Fig. S6). Seasonally, high  $\text{CO}_2$  emission flux occurred in spring and winter for

both subzones (Fig. S6). The average CO<sub>2</sub> emission flux was  $42.1 \pm 44.8 \text{ mmol m}^{-2} \text{ d}^{-1}$  across the three subzones.

## Discussion

### Changes in CO<sub>2</sub> and the role of eutrophication

The lake has experienced eutrophication due to human-driven pollutant discharge by inflowing rivers (Qin et al. 2007). The large differences in *p*CO<sub>2</sub> and associated CO<sub>2</sub> flux between the river mouth and other subzones (Fig. S5) supported the interpretation that human-induced external input plays an important role in lake CO<sub>2</sub> emissions. The river mouth had the highest nutrient and DOC concentrations (Table S1) due to high human-driven river discharge, which has been demonstrated by previous studies (Qin et al. 2007; Xu et al. 2017; Xiao et al. 2020b) and our field samplings (Fig. S7). These high external inputs can increase *p*CO<sub>2</sub> by increasing respiration and organic matter degradation (Sobek et al. 2005; Kortelainen et al. 2006). Importantly, higher *p*CO<sub>2</sub> in inflowing rivers also controlled the *p*CO<sub>2</sub> variability in river mouths (Fig. S7c), indicating that the direct external input of CO<sub>2</sub> may significantly fuel the CO<sub>2</sub> level (Stets et al. 2009; Weyhenmeyer et al. 2015; Wilkinson et al. 2016). Thus, significantly higher CO<sub>2</sub> in the river mouth can be interpreted as a consequence of external nutrient and carbon input from the watershed, which would stimulate microbial activities and enhance respiration, resulting in more CO<sub>2</sub> production (Sobek et al. 2005; Kortelainen et al. 2006; Zhang et al. 2021).

The large interannual variability in CO<sub>2</sub> also indicated the impact of anthropogenic eutrophication. From 1992 to 1995, the increasing *p*CO<sub>2</sub> mostly resulted from the increase in external input due to rapid industrial expansion and population growth in the Lake Taihu catchment (Xu et al. 2017), which could be seen in the increasing lake nutrient concentrations (Figs. 2, S2). We proposed that high nutrient loadings may stimulate mineralization and increase CO<sub>2</sub> production, which had been shown in previous studies (Kortelainen et al. 2006; Perga et al. 2016; Wang et al. 2017). Between 1996 and 2001, the decline in *p*CO<sub>2</sub> could be explained by the decrease in external pollutant input due to watershed management (Paerl et al. 2011). However, external input via rivers increased again after 2001 (Xu et al. 2017; Xiao et al. 2020a), probably leading to increasing *p*CO<sub>2</sub> (Fig. 2). In Lake Taihu, serious algal blooms in 2007 caused a highly publicized drinking water crisis, prompting a wide range of activities to reduce external pollutant inputs (Qin et al. 2019). These measures may have directly led to the decline in *p*CO<sub>2</sub> and associated CO<sub>2</sub> flux after 2007. The high sensitivity of lake CO<sub>2</sub> dynamics to external input has been reported in other lakes worldwide via measurements and modeling (Maberly et al. 2013; Weyhenmeyer et al. 2015; Kiuru et al. 2018), suggesting that changes in human-driven eutrophication play an important role in altering lake CO<sub>2</sub> budgets via affecting internal metabolic activities (e.g., respiration) and external loading input.

Previous studies have shown that lake eutrophication can cause either an increase (Kortelainen et al. 2006; Morales-Williams et al. 2021) or a decrease (Balmer and Downing 2011; Pacheco et al. 2014) in *p*CO<sub>2</sub>, leading to a large uncertainty in evaluating the effects. Similarly, our study showed that *p*CO<sub>2</sub> increased in the river mouth corresponding to an increasing TSI, the index of eutrophication status; in contrast, it decreased in Meiliang Bay with an increasing TSI (Fig. 5). The two subzones were both eutrophic with nonsignificant ( $p > 0.05$ ) differences in TSI and Chl *a*. The river mouth received high external inputs of nutrients and CO<sub>2</sub> via rivers (Fig. S7), which not only increased TSI but also increased *p*CO<sub>2</sub>, leading to *p*CO<sub>2</sub> covarying with TSI in the same direction. Chl *a* dominated the TSI in Meiliang Bay without direct internal input (Fig. 5b), likely leading to a decrease in *p*CO<sub>2</sub> with increasing TSI due to high primary production (Balmer and Downing 2011; Pacheco et al. 2014). Previous studies found that the effects of eutrophication on *p*CO<sub>2</sub> varied among lakes (Kortelainen et al. 2006; Marotta et al. 2010; Balmer and Downing 2011). Considering the river mouth and Meiliang Bay were both eutrophic, our results suggest that the effects can vary among subzones within a single lake, which was linked to external input and in-lake primary production.

### Temperature influences on CO<sub>2</sub> variations

Long-term sampling showed that *p*CO<sub>2</sub> decreased with increasing water temperature (Fig. 6; Table 1). This finding was consistent with long-term field measurements from boreal lakes (Finlay et al. 2015) and with the longest lake mesocosm experiment in Denmark (Davidson et al. 2015), showing a decrease in *p*CO<sub>2</sub> with warming. However, it should be noted that a previous study also reported that warming increased lake CO<sub>2</sub> production (Kosten et al. 2010). Temperature is related to the variability of a series of abiotic and biotic parameters (e.g., primary production, respiration, and nutrient availability), which are associated with lake CO<sub>2</sub> consumption and production (Gudasz et al. 2010; Kosten et al. 2012; Davidson et al. 2015). Thus, the temperature effect may be related to these factors, probably leading to warming could either increase lake CO<sub>2</sub> emission via stimulating respiration or decrease emission via promoting primary production.

Here, both analyses identified that temperate-induced algal blooms caused a decrease in lake *p*CO<sub>2</sub> (Figs. 3, 4). Algal blooms played an important role in lake CO<sub>2</sub> uptake (Balmer and Downing 2011; Pacheco et al. 2014), leading to significant negative correlation between *p*CO<sub>2</sub> and Chl *a* (an index of algal blooms; Fig. 4). Algal blooms in the lake were boosted by a warmer climate (Duan et al. 2009; Qin et al. 2019), and seasonal variation in Chl *a* was consistent with temperature (Fig. 3). Lower *p*CO<sub>2</sub> occurred in warm seasons with higher Chl *a* and it peaked in cold seasons with lower Chl *a*, and the *p*CO<sub>2</sub> seasonal variation was more profound in the river mouth and Meiliang Bay with high Chl *a* (Figs. 3, S3), suggesting the indirect effect of temperature related to primary

production (Davidson et al. 2015). Specifically, a nonsignificant ( $p > 0.05$ ) water temperature difference between spring (16.4°C) and autumn (19.7°C) was found in this study; however, a significantly ( $p < 0.05$ ) lower  $p\text{CO}_2$  in autumn was observed, mostly due to the significantly ( $p < 0.05$ ) higher Chl *a* at that time. It is likely that temperature controls the seasonal variation in Chl *a* (Fig. 3), which in turn influences the seasonal variations in  $p\text{CO}_2$ .

However, the temperature effects reported here varied spatially and temporally. Although the seasonal variation in temperature was remarkably uniform across the three subzones and the four periods (Figs. 3, S3), temperature played a smaller role in the river mouth with significant external loadings and during 2002–2006 with high nutrient loadings (Fig. 6; Table 1). Considering the significant correlations between  $p\text{CO}_2$  and  $\text{NH}_4^+\text{-N}$ , TN, and DOC (Fig. 4; Table S2), our results are consistent with a long-term mesocosm experiment and with a global-scale database, showing that nonthermal factors (e.g., nutrient and dissolved carbon fraction) may confound the temperature effect on  $p\text{CO}_2$  (Sobek et al. 2005; Davidson et al. 2015). Meanwhile, the temperature effects were negatively correlated with the ratio of TN to TP and positively correlated with the ratio of Chl *a* to TN (Fig. S4). Considering that the temperature could increase CO<sub>2</sub> consumption via stimulating algal blooms and N loadings could increase CO<sub>2</sub> production via stimulating respiration as shown above, our results suggested that the temperature effect could be amplified with decreasing N loading and increasing Chl *a* mostly due to CO<sub>2</sub> consumption override those of production.

### Implications of the lake CO<sub>2</sub> budget

Temporal and spatial variability in CO<sub>2</sub> within lakes has received considerable attention to accurately estimate the CO<sub>2</sub> budget (Natchimuthu et al. 2017; Loken et al. 2019; Xiao et al. 2020a). Our results showed large  $p\text{CO}_2$  and CO<sub>2</sub> fluxes occurred in the river mouth with high external input. It is estimated that lake littoral zone or river mouth CO<sub>2</sub> emissions in eastern China were approximately 1.4 times higher than those in open water (Li et al. 2018), and the magnitude was approximately 8 in this study. Meanwhile, the lowest  $p\text{CO}_2$  and CO<sub>2</sub> fluxes occurred in the summer and peaked in the winter due to the seasonal variations in temperate-related primary production (Figs. 3, S6), which is consistent with a field survey in eutrophic Lake Donghu in a subtropical climate (Xing et al. 2005) and with a study in 151 temperate lakes (Trolle et al. 2012). Thus, our results reported here suggest efflux estimates either excluding river mouths with high external input or focusing on warm seasons with high primary production may underestimate lake CO<sub>2</sub> emissions. These further emphasized the importance of considering spatiotemporal variability in CO<sub>2</sub> to obtain unbiased lake flux (Natchimuthu et al. 2017; Klaus et al. 2019).

A highly dynamic role of the lake as atmospheric CO<sub>2</sub> source was found in our study. Specifically, a significantly

decreasing trend in annual CO<sub>2</sub> emissions was presented over the 24-yr study (1992–2015). Our results found nutrient concentrations affect the lake  $p\text{CO}_2$  and CO<sub>2</sub> flux variability on an interannual scale (Figs. 2, S6), which is consistent with a study that reconstructed long-term  $p\text{CO}_2$  using paleolimnological data (Perga et al. 2016). Both of these suggest that the substantial interannual variability in CO<sub>2</sub> was partly explained by the changing nutrient loading. It is worth to note that large interannual variability in inland water nutrient loadings have been found (Zhou et al. 2017; Fig. S2), suggesting the importance of long-term measurements to accurately estimate lake CO<sub>2</sub> budgets and better understand their roles in the carbon cycle. For example, the CO<sub>2</sub> emission flux of the eutrophic part of the lake was estimated to be 30 mmol m<sup>-2</sup> d<sup>-1</sup> based on measurements from 2000 to 2015 (Xiao et al. 2020a), which was lower than the value in the presented study (42.1 mmol m<sup>-2</sup> d<sup>-1</sup>).

The warming rate of the lake was 0.35°C per decade, which was similar to the average rate of global lakes (Woolway et al. 2020). Our results showed that the  $p\text{CO}_2$  and CO<sub>2</sub> fluxes decreased with increasing temperature, especially for Meiliang Bay, which is affected by frequent algal blooms. Meanwhile, the temperature effect was amplified with an increasing ratio of Chl *a* to TN. Decreasing lake N loadings have been reported due to environmental protection actions to improve water quality (Zhou et al. 2017; Qin et al. 2019), but algal blooms have increased with climate warming (Kosten et al. 2012; Ho et al. 2019). Considering the significant role of algal blooms in lake CO<sub>2</sub> variability (Balmer and Downing 2011; Pacheco et al. 2014), future warmer climate would have a large role in lake CO<sub>2</sub> flux via stimulating algal blooms.

It is worth to note that there are several limitations in our study. First, significant temporal variation of CO<sub>2</sub> was observed, future studies should conduct field sampling with a greater frequency to better understanding the drivers of lake CO<sub>2</sub> variability. Second, our results showed peak  $p\text{CO}_2$  and CO<sub>2</sub> flux occurred in river mouth with large external loading, and quantifying the rates of nutrient and carbon inputs from watershed can provide useful information to explain the CO<sub>2</sub> variability. Third, we found that eutrophication and warming both drove lake CO<sub>2</sub> variability, future studies should investigate the interactive effects on CO<sub>2</sub> variability to accurately predict future emissions. Lastly, this study only looked at CO<sub>2</sub> dynamics but to have a more holistic picture of carbon gas emissions in the lake future studies should also consider CH<sub>4</sub> dynamics, which have been shown to be impacted by nutrients and warming (Xing et al. 2005; Denfeld et al. 2016; Xiao et al. 2017).

### Conclusions

Long-term (1992–2015) sampling at the monthly scale showed that the  $p\text{CO}_2$  and CO<sub>2</sub> fluxes varied spatially, seasonally, and annually. The highest  $p\text{CO}_2$  and CO<sub>2</sub> fluxes occurred in the river mouth due to substantial external input. Lower  $p\text{CO}_2$  and CO<sub>2</sub> fluxes were found in the warm season with

high Chl *a*. The most notable feature was that the *p*CO<sub>2</sub> and CO<sub>2</sub> fluxes varied greatly over 24 yr, much longer than in previous results, suggesting the importance of long-term field measurements to achieve unbiased results.

Eutrophication caused by nutrient enrichment controlled the variability of *p*CO<sub>2</sub> and CO<sub>2</sub> fluxes on decadal scales. Temperature drove the seasonal variation in CO<sub>2</sub> emissions by stimulating primary production, especially for eutrophic lakes. Our results reported here suggest that eutrophication and warming both drove lake CO<sub>2</sub> variability.

## References

- Abril, G., and others. 2015. Technical note: Large overestimation of *p*CO<sub>2</sub> calculated from pH and alkalinity in acidic, organic-rich freshwaters. *Biogeosciences* **12**: 67–78. doi:10.5194/bg-12-67-2015
- Balmer, M. B., and J. A. Downing. 2011. Carbon dioxide concentrations in eutrophic lakes: Undersaturation implies atmospheric uptake. *Inland Waters* **1**: 125–132. doi:10.5268/IW-1.2.366
- Bastviken, D., J. Ejlerstsson, and L. Tranvik. 2002. Measurement of methane oxidation in lakes: A comparison of methods. *Environ. Sci. Technol.* **36**: 3354–3361. doi:10.1021/es010311p
- Cole, J. J., and N. F. Caraco. 1998. Atmospheric exchange of carbon dioxide in a low-wind oligotrophic lake measured by the addition of SF<sub>6</sub>. *Limnol. Oceanogr.* **43**: 647–656. doi:10.4319/lo.1998.43.4.0647
- Cole, J. J., and others. 2007. Plumbing the global carbon cycle: Integrating inland waters into the terrestrial carbon budget. *Ecosystems* **10**: 171–184. doi:10.1007/s10021-006-9013-8
- Davidson, T. A., and others. 2015. Eutrophication effects on greenhouse gas fluxes from shallow lake mesocosms override those of climate warming. *Glob. Chang. Biol.* **21**: 4449–4463. doi:10.1111/gcb.13062
- Denfeld, B. A., M. Ricão Canelhas, G. Weyhenmeyer, S. Bertilsson, A. Eiler, and D. Bastviken. 2016. Constraints on methane oxidation in ice-covered boreal lakes. *J. Geophys. Res. Biogeosci.* **121**: 1924–1933. doi:10.1002/2016JG003382
- Duan, H. T., and others. 2009. Two-decade reconstruction of algal blooms in China's Lake Taihu. *Environ. Sci. Technol.* **43**: 3522–3528. doi:10.1021/es8031852
- Finlay, K., R. J. Vogt, G. L. Simpson, and P. R. Leavitt. 2019. Seasonality of *p*CO<sub>2</sub> in a hard-water lake of the northern Great Plains: The legacy effects of climate and limnological conditions over 36 years. *Limnol. Oceanogr.* **64**: S118–S129. doi:10.1002/lno.11113
- Finlay, K., and others. 2015. Decrease in CO<sub>2</sub> efflux from northern hardwater lakes with increasing atmospheric warming. *Nature* **519**: 215–218. doi:10.1038/nature14172
- Gudasz, C., D. Bastviken, K. Steger, K. Premke, S. Sobek, and L. J. Tranvik. 2010. Temperature-controlled organic carbon mineralization in lake sediments. *Nature* **466**: 478–482. doi:10.1038/nature09186
- Ho, J. C., A. M. Michalak, and N. Pahlevan. 2019. Widespread global increase in intense lake phytoplankton blooms since the 1980s. *Nature* **574**: 667–670. doi:10.1038/s41586-019-1648-7
- Kiuru, P., and others. 2018. Effects of climate change on CO<sub>2</sub> concentration and efflux in a humic boreal lake: A modeling study. *Eur. J. Vasc. Endovasc. Surg.* **123**: 2212–2233. doi:10.1029/2018JG004585
- Klaus, M., D. A. Seekell, W. Lidberg, and J. Karlsson. 2019. Evaluations of climate and land management effects on lake carbon cycling need to account for temporal variability in CO<sub>2</sub> concentrations. *Global Biogeochem. Cycles* **33**: 243–265. doi:10.1029/2018GB005979
- Kortelainen, P., and others. 2006. Sediment respiration and lake trophic state are important predictors of large CO<sub>2</sub> evasion from small boreal lakes. *Glob. Chang. Biol.* **12**: 1554–1567. doi:10.1111/j.1365-2486.2006.01167.x
- Kosten, S., and others. 2010. Climate-dependent CO<sub>2</sub> emissions from lakes. *Global Biogeochem. Cycles* **24**: GB2007. doi:10.1029/2009GB003618
- Kosten, S., and others. 2012. Warmer climates boost cyanobacterial dominance in shallow lakes. *Glob. Chang. Biol.* **18**: 118–126. doi:10.1111/j.1365-2486.2011.02488.x
- Lee, X., and others. 2014. The Taihu Eddy Flux Network: An observational program on energy, water, and greenhouse gas fluxes of a large freshwater lake. *Bull. Am. Meteorol. Soc.* **95**: 1583–1594. doi:10.1175/bams-d-13-00136.1
- Li, S., and others. 2018. Large greenhouse gases emissions from China's lakes and reservoirs. *Water Res.* **147**: 13–24. doi:10.1016/j.watres.2018.09.053
- Loken, L. C., J. T. Crawford, P. J. Schramm, P. Stadler, A. R. Desai, and E. H. Stanley. 2019. Large spatial and temporal variability of carbon dioxide and methane in a eutrophic lake. *Eur. J. Vasc. Endovasc. Surg.* **124**: 2248–2266. doi:10.1029/2019JG005186
- Maberly, S. C., P. A. Barker, A. W. Stott, and M. M. De Ville. 2013. Catchment productivity controls CO<sub>2</sub> emissions from lakes. *Nat. Clim. Change* **3**: 391–394. doi:10.1038/NCLIMATE1748
- Marotta, H., C. M. Duarte, F. Meirelles-Pereira, L. Bento, F. A. Esteves, and A. Enrich-Prast. 2010. Long-term CO<sub>2</sub> variability in two shallow tropical lakes experiencing episodic eutrophication and acidification events. *Ecosystems* **13**: 382–392. doi:10.1007/s10021-010-9325-6
- Morales-Williams, A. M., A. D. Wanamaker, C. J. Williams, and J. A. Downing. 2021. Eutrophication drives extreme seasonal CO<sub>2</sub> flux in lake ecosystems. *Ecosystems* **24**: 434–450. doi:10.1007/s10021-020-00527-2
- Natchimuthu, S., I. Sundgren, M. Galfalk, L. Klemedtsson, and D. Bastviken. 2017. Spatiotemporal variability of lake *p*CO<sub>2</sub> and CO<sub>2</sub> fluxes in a hemiboreal catchment. *Eur. J. Vasc. Endovasc. Surg.* **122**: 30–49. doi:10.1002/2016JG003449
- Pacheco, F. S., F. Roland, and J. A. Downing. 2014. Eutrophication reverses whole-lake carbon budgets. *Inland Waters* **4**: 41–48. doi:10.5268/IW-4.1.614

- Paerl, H. W., and V. J. Paul. 2012. Climate change: Links to global expansion of harmful cyanobacteria. *Water Res.* **46**: 1349–1363. doi:10.1016/j.watres.2011.08.002
- Paerl, H. W., and others. 2011. Controlling harmful cyanobacterial blooms in a hypereutrophic lake (Lake Taihu, China): The need for a dual nutrient (N & P) management strategy. *Water Res.* **45**: 1973–1983. doi:10.1016/j.watres.2010.09.018
- Perga, M.-E., S. C. Maberly, J.-P. Jenny, B. Alric, C. Pignol, and E. Naffrechoux. 2016. A century of human-driven changes in the carbon dioxide concentration of lakes. *Global Biogeochem. Cycles* **30**: 93–104. doi:10.1002/2015GB005286
- Qi, T., and others. 2020. Satellite estimation of dissolved carbon dioxide concentrations in China's Lake Taihu. *Environ. Sci. Technol.* **54**: 13709–13718. doi:10.1021/acs.est.0c04044
- Qin, B., P. Xu, Q. Wu, L. Luo, and Y. Zhang. 2007. Environmental issues of Lake Taihu, China. *Hydrobiologia* **581**: 3–14. doi:10.1007/s10750-006-0521-5
- Qin, B., and others. 2019. Why Lake Taihu continues to be plagued with cyanobacterial blooms through 10 years (2007–2017) efforts. *Sci. Bull.* **64**: 354–356. doi:10.1016/j.scib.2019.02.008
- Raymond, P. A., and others. 2013. Global carbon dioxide emissions from inland waters. *Nature* **503**: 355–359. doi:10.1038/nature12760
- Seekell, D. A., and C. Gudasz. 2016. Long-term pCO<sub>2</sub> trends in Adirondack Lakes. *Geophys. Res. Lett.* **43**: 5109–5115. doi:10.1002/2016GL068939
- Sobek, S., L. J. Tranvik, and J. J. Cole. 2005. Temperature independence of carbon dioxide supersaturation in global lakes. *Global Biogeochem. Cycles* **19**: GB2003. doi:10.1029/2004GB002264
- Stets, E., R. Striegl, G. Aiken, D. Rosenberry, and T. Winter. 2009. Hydrologic support of carbon dioxide flux revealed by whole-lake carbon budgets. *J. Geophys. Res.* **114**: G01008. doi:10.1029/2008JG000783
- Tranvik, L. J., and others. 2009. Lakes and reservoirs as regulators of carbon cycling and climate. *Limnol. Oceanogr.* **54**: 2298–2314. doi:10.4319/lo.2009.54.6\_part\_2.2298
- Trolle, D., and others. 2012. Seasonal dynamics of CO<sub>2</sub> flux across the surface of shallow temperate lakes. *Ecosystems* **15**: 336–347. doi:10.1007/s10021-011-9513-z
- Wang, X., and others. 2017. pCO<sub>2</sub> and CO<sub>2</sub> fluxes of the metropolitan river network in relation to the urbanization of Chongqing, China. *J. Geophys. Res. Biogeosci.* **122**: 470–486. doi:10.1002/2016JG003494
- Weyhenmeyer, G. A., S. Kosten, M. B. Wallin, L. J. Tranvik, E. Jeppesen, and F. Roland. 2015. Significant fraction of CO<sub>2</sub> emissions from boreal lakes derived from hydrologic inorganic carbon inputs. *Nat. Geosci.* **8**: 933–936. doi:10.1038/NNGEO2582
- Wilkinson, G. M., C. D. Buelo, J. J. Cole, and M. L. Pace. 2016. Exogenously produced CO<sub>2</sub> doubles the CO<sub>2</sub> efflux from three north temperate lakes. *Geophys. Res. Lett.* **43**: 1996–2003. doi:10.1002/2016GL067732
- Woolway, R. I., B. M. Kraemer, J. D. Lenters, C. J. Merchant, C. M. O'Reilly, and S. Sharma. 2020. Global lake responses to climate change. *Nat. Rev. Earth Environ.* **1**: 388–403. doi:10.1038/s43017-020-0067-5
- Xiao, Q., and others. 2017. Spatial variations of methane emission in a large shallow eutrophic lake in subtropical climate. *Eur. J. Vasc. Endovasc. Surg.* **122**: 1597–1614. doi:10.1002/2017JG003805
- Xiao, Q., and others. 2019. Coregulation of nitrous oxide emissions by nitrogen and temperature in China's third largest freshwater lake (Lake Taihu). *Limnol. Oceanogr.* **64**: 1070–1086. doi:10.1002/lno.11098
- Xiao, Q., and others. 2020a. Eutrophic Lake Taihu as a significant CO<sub>2</sub> source during 2000–2015. *Water Res.* **170**: 115331. doi:10.1016/j.watres.2019.115331
- Xiao, Q., and others. 2020b. Environmental investments decreased partial pressure of CO<sub>2</sub> in a small eutrophic urban lake: Evidence from long-term measurements. *Environ. Pollut.* **263**: 114433. doi:10.1016/j.envpol.2020.114433
- Xiao, W., and others. 2014. A flux-gradient system for simultaneous measurement of the CH<sub>4</sub>, CO<sub>2</sub>, and H<sub>2</sub>O fluxes at a lake-air interface. *Environ. Sci. Technol.* **48**: 14490–14498. doi:10.1021/es5033713
- Xing, Y. P., P. Xie, H. Yang, L. Y. Ni, Y. S. Wang, and K. W. Rong. 2005. Methane and carbon dioxide fluxes from a shallow hypereutrophic subtropical Lake in China. *Atmos. Environ.* **39**: 5532–5540. doi:10.1016/j.atmosenv.2005.06.010
- Xu, H., H. W. Paerl, G. Zhu, B. Qin, N. S. Hall, and M. Zhu. 2017. Long-term nutrient trends and harmful cyanobacterial bloom potential in hypertrophic Lake Taihu, China. *Hydrobiologia* **787**: 229–242. doi:10.1007/s10750-016-2967-4
- Zhang, Y., B. Qin, G. Zhu, K. Shi, and Y. Zhou. 2018a. Profound changes in the physical environment of Lake Taihu from 25 years of long-term observations: Implications for algal bloom outbreaks and aquatic macrophyte loss. *Water Resour. Res.* **54**: 4319–4331. doi:10.1029/2017WR022401
- Zhang, Y., Y. Zhou, K. Shi, B. Qin, X. Yao, and Y. Zhang. 2018b. Optical properties and composition changes in chromophoric dissolved organic matter along trophic gradients: Implications for monitoring and assessing lake eutrophication. *Water Res.* **131**: 255–263. doi:10.1016/j.watres.2017.12.051
- Zhang, Y., and others. 2021. Spatial variations in CO<sub>2</sub> fluxes in a subtropical coastal reservoir of Southeast China were related to urbanization and land-use types. *J. Environ. Sci.* **109**: 206–218. doi:10.1016/j.jes.2021.04.003
- Zhou, Y., and others. 2017. Improving water quality in China: Environmental investment pays dividends. *Water Res.* **118**: 152–159. doi:10.1016/j.watres.2017.04.035

### Acknowledgments

We are grateful for the constructive comments from the journal reviewers, the editors Edward Stets and Julia Mullarney. We would like to thank the Taihu Laboratory for Lake Ecosystem Research (TLLER) for providing the observational data. The study was funded jointly by the National Natural Science Foundation of China (41801093 and 41971309) and the Research Startup Project of Nanjing Institute of Geography and Limnology, Chinese Academy of Sciences (NIGLAS2019QD007).

### Conflict of interest

None declared.

*Submitted 16 April 2021*

*Revised 27 October 2021*

*Accepted 29 November 2021*

*Associate editor: Edward G. Stets*